Myb-binding Protein 1a (Mybbp1a) Regulates Levels and Processing of Pre-ribosomal RNA*

Julia Hochstatter[1,3], Michael Hölzel[2,7], Michaela Rohrmoser[2], Lothar Schermelleh[6], Heinrich Leonhardt[6], Rebecca Keough[4], Thomas J. Gonda[5], Axel Imhof[3], Dirk Eick[2], Gernot Längst[1] and Attila Németh[1]

[1]Biochemistry Center Regensburg, University of Regensburg, Universitätsstr. 31, 93053 Regensburg, Germany

[2]Department of Molecular Epigenetics, Helmholtz Center Munich and Center of Integrated Protein Science Munich (CIPSM), 81377 Munich, Germany

[3]Adolf-Butenandt Institute and Munich Center of Integrated Protein Science (CIPSM), Ludwig Maximilians University of Munich, 80336 Munich, Germany

[4]School of Medicine, Flinders University, Adelaide 5001, Australia

[5]Diamantina Institute for Cancer, Immunology and Metabolic Medicine, University of Queensland Research Wing, Building 1, Princess Alexandra Hospital Campus, Ipswich Road, Buranda, Queensland 4102 Australia

[6]Department of Biology and Center for Integrated Protein Science, Ludwig Maximilians University of Munich, Grosshaderner Str. 2, 82152 Planegg-Martinsried, Germany

[7]Present address: Institute of Clinical Chemistry and Clinical Pharmacology, University Hospital Bonn, Bonn, Germany

*Running title: *Coordination of rRNA gene transcription and processing*

To whom correspondence should be addressed: Gernot Längst and Attila Németh, Biochemistry Center Regensburg, University of Regensburg, Universitätsstr. 31, 93053 Regensburg, Germany. Tel.: 49-(0)941-943 2849; Fax: 49-(0)941-943 2474; E-mail: gernot.laengst@vkl.uni-regensburg.de, attila.nemeth@vkl.uni-regensburg.de

Keywords: gene regulation; nucleolus; ribosomal RNA (rRNA); rRNA processing; transcription regulation

Background: rRNA gene transcription and processing have to be coordinated, as they are intimately linked.
Results: Mybbp1a regulates RNA Pol I transcription and pre-rRNA processing.
Conclusion: Mybbp1a coordinates both processes.
Significance: Mybbp1a was shown to be an important regulator of cellular proliferation, related to RNA Pol II genes. We link its function now as well to regulating RNA Pol I genes and to control ribosome biogenesis.

SUMMARY

Ribosomal RNA gene transcription, co-transcriptional processing and ribosome biogenesis are highly coordinated processes that are tightly regulated during cell growth. In this study, we discovered that Mybbp1a is associated with both the RNA Polymerase I (RNA Pol I) complex and the ribosome biogenesis machinery. Using a reporter assay that uncouples transcription and RNA processing, we show that Mybbp1a represses rRNA gene transcription. In addition, overexpression of the protein reduces RNA Pol I loading on endogenous rRNA genes as revealed by chromatin immunoprecipitation experiments. Accordingly, depletion of Mybbp1a results in an accumulation of the rRNA precursor *in vivo* but surprisingly causes also growth arrest of the cells. This effect can be explained by the observation that the modulation of Mybbp1a protein levels results in defects in pre-rRNA processing within the cell. Therefore, the protein may play a dual role in the rRNA metabolism, potentially linking and coordinating ribosomal DNA (rDNA)

transcription and pre-rRNA processing to allow for the efficient synthesis of ribosomes.

Cellular growth and division is tightly coupled to ribosome synthesis, a major cellular undertaking that is energetically very costly (reviewed in (1)). This process requires the matched activity of the three forms of RNA polymerase to produce the building blocks of the ribosomes and the coordinated expression, processing and assembly of the pre-rRNA into ribosomes (2,3).

Mammalian cells contain 300 to 400 rRNA gene repeats, most of which are arranged as tandem repeats. The level of rRNA synthesis in the cell is determined by the dynamic regulation of about half of those genes, whereas the remaining genes are constantly repressed (4). Active and inactive gene populations are discriminated by different epigenetic states and different topological conformations (5-7). The expression levels of the active portion of the rRNA genes are tightly regulated in accordance with the physiological condition of the cell. Various signal transduction pathways, including the mTOR pathway and the MAPK cascade, directly target different steps of rRNA synthesis to efficiently regulate the production of ribosomes. Several post-translational modifications of the Pol I-specific transcription initiation factor TIF-IA and the rDNA transcription factor UBF have been characterised, and their impacts on transcriptional pre-initiation complex (PIC) formation and/or elongation have been shown (8-11).

The localisation of ribosome biogenesis to the nucleolus and the close juxtaposition of the factors involved in transcription, processing and ribosome assembly, as revealed by microscopy techniques, suggest that these processes are directly coupled. Co-transcriptional processing of the pre-rRNA transcript was recently shown by EM visualisation of nascent rRNA transcripts. The 5' terminal knobs, containing U3 snoRNA and associated Utps (U three proteins), increased in size with transcript length, indicating that rRNA processing, RNA folding, RNA modification and ribosomal protein assembly also occur co-transcriptionally (12-15).

Early rRNA processing is initiated by the assembly of the small ribosome subunit (SSU) processome complex, which contains U3 snoRNA (14) that base pairs with sequences near the 5' end of the pre-rRNA. SSU processome-dependent processing leads to rRNA cleavage and the release of the small subunit rRNA (18S) from the ribosome (13). A subset of seven SSU processome proteins, the t-Utps (transcriptional-Utps), is also required for efficient rDNA transcription in yeast, linking rDNA transcription with rRNA processing and ribosome assembly (2). McStay and co-workers have identified the human orthologs of the t-Utps and confirmed their requirement for both efficient transcription and processing of the 47S pre-rRNA (16), indicating that this coordinated mechanism is conserved throughout evolution. Their study further revealed that the t-Utps are recruited to rDNA, irrespective of the transcription status of the rDNA gene.

Recently, Moss and colleagues have suggested a role for transcription elongation in rRNA processing and ribosome assembly (17). Erk-dependent phosphorylation of UBF directly influences RNA Pol I elongation rates by inducing an UBF-dependent rearrangement of the chromatin environment. This effect could serve as a mechanism to coordinate transcription and the assembly of pre-ribosomal complexes on nascent rRNA by modulating the Pol I elongation rate. Further insights into how these processes might be coordinated came from Nomura and co-workers who demonstrated a physical interaction of Pol I with the elongation factors Spt4 and Spt5 and an rRNA processing defect upon depletion of the latter (18). A connection between transcription elongation and rRNA processing was further confirmed by using a yeast strain with a mutated RNA Pol I enzyme with reduced elongation rates (3). Reduced elongation rates lead to severe defects in rRNA processing and ribosome assembly, suggesting an intimate link between elongation rates and rRNA maturation. Thus, ribosome biogenesis appears to be controlled by feedback mechanisms, which ensure that proper assembly occurs on all synthesis levels, from transcription initiation to ribosome export.

The expression of the rRNA genes is regulated at different levels of the rRNA metabolic pathway, at the stage of transcription initiation (reviewed in (19)), transcription elongation (17,18), rRNA processing and assembly (20-22). To identify novel regulators of rRNA gene synthesis, we screened for factors interacting with RNA Pol I. We identified Myb-binding protein 1a (Mybbp1a), which is ubiquitously expressed and predominantly localises to the nucleolus (23,24). The 160-kDa Mybbp1a protein had originally been described as an interacting partner of the proto-oncogene c-Myb and since then it has been shown to interact with and to modulate the activity of several regulators of Pol II-dependent transcription. In certain myeloid cell types, the protein is post-translationally processed to generate an N-terminal fragment of 67 kDa ($p67^{MBP}$) (23). Mybbp1a, and in some cases also $p67^{MBP}$, have been described to interact with several other transcriptional regulators, such as PPAR gamma coactivator 1α (PGC-1α), NF-κB, aromatic hydrocarbon receptor (AhR), Prep1 and CRY1, and linked to diverse cellular processes (e.g. mitochondrial biogenesis, cell proliferation, apoptosis etc.) by modulating the activity of these regulators (25-29).

Despite its predominant localisation to the nucleolus, the function of Mybbp1a in this cellular compartment remained largely unclear. The data shown here demonstrate two new functions for Mybbp1a in the nucleolus. It associates with the RNA Pol I machinery and is able to repress its transcriptional activity.

EXPERIMENTAL PROCEDURES

DNA constructs - To generate a Flag-tagged RPA116 expression construct the coding sequence of mouse RPA116 was amplified from the cDNA clone pBS-RPA 116 6-2 (kindly provided by I. Grummt; (30)) using the following primer pair in a standard PCR with the Expand High Fidelity system (Roche). The forward (5'-ATG GAT CCA TGG ACT ACA AGG ACG ACG ATG ACA AGG ATG TCG ACG GCC GG-3') and reverse primer (5'-GAG GAT CCT CAG ATG ACA TCC AGT TTC ACT-3') introduced a Flag coding sequence upstream of the RPA116 ORF. The PCR product was cloned into pEGZ (pEGZ-fRPA116).

The human Flag-Mybbp1a expression construct was generated by PCR amplification of the human Mybbp1a cDNA clone described previously (31) using Pfu DNA Polymerase (Promega). The forward primer (5'-AG TCA AGC TTC ACC ATG GAC TAC AAG GAC GAC GAT GAC AAG GAG AGC CGG GAT CCC GCC-3') introduced an N-terminal Flag-tag and Nco I restriction site at the initiation codon and the reverse primer (5'-GCT CTA GAT CAG GGT TTC CCT GCC TTC-3') introduced an Xba I restriction site at the stop codon to facilitate cloning into the pact expression vector, as used previously (23). The mouse Flag-Mybbp1a (mMybbp1a), mouse Flag-$p67^{MBP}$*NLS (Flag-$mp67^{MBP}$*) and the human Flag-Tip5 have been previously described (Tavner *et al.* 1998; Keough *et al.* 2003(32). GFP-RPA43 was obtained from Addgene (Addgene plasmid 17659).

Cell culture and proliferation assay - The mouse lymphoblast cell line MB III (ATCC® Number: CCL-32™) was cultured in MEM (Earles, with Glutamax) with non-essential amino acids, sodium pyruvate (110 mg/L) and 10% heat-inactivated newborn calf serum (Invitrogen). To create a MB III cell line stably expressing Flag-RPA116, cells were transfected with pEGZ-fRPA116, selected with Zeocin (Invitrogen), cloned by serial dilution and then further maintained with 100 μg/ml Zeocin. HeLa cells were cultured in DMEM containing 10% heat-inactivated fetal calf serum (FCS, Invitrogen) and Penicillin/Streptomycin. Both cell lines were cultured at 37 °C in 5% CO_2.

To monitor proliferation rates HeLa cells were detached with Trypsin-EDTA and diluted in PBS. Subsequently cells were stained with trypan blue and living cells were counted.

Preparation of cellular extracts and immunopurification of proteins - To prepare nuclear extracts MB III and Flag-RPA116-MB III cells were harvested, washed with PBS and resuspended in 3 packed cell volumes (PCV) of buffer A (20 mM, HEPES pH 7.9; 0.2% NP-40; 10 mM KCl; 1 mM EDTA; 10% Glycerol; 1 mM DTT; protease inhibitors), incubated on ice for 10 min. Cell lysis was followed by microscopy. Nuclei were washed in Buffer A, resuspended in 3 PCV of Buffer B (420 mM NaCl; 20 mM; HEPES pH 7.9; 10 mM KCl; 1 mM EDTA; protease inhibitors) containing 2% (v/v) Distamycin A hydrochloride (Sigma, D6135) and incubated on a rotating wheel at 4°C for 40 min. After centrifugation the nuclear fraction was collected and dialysed against AM100 (100 mM NaCl; 20 mM Tris HCl, pH 7.9; 5 mM $MgCl_2$; 0.1 mM EDTA; 20% Glycerol; 1 mM DTT; protease inhibitors).

HEK293T nuclear extracts were prepared 48 h after transfection with Flag-Mybbp1a or empty vector control as described above.

HeLa nuclear extracts were prepared 48 h after transfection with Flag-Mybbp1a or vector control. Cells were detached by Trypsin-EDTA (Invitrogen), washed with PBS, centrifuged at 2.500 g for 5 min and resuspended in 5xPCV of Buffer C (10 mM KCl; 10 mM HEPES, pH 7.9; 1.5 mM $MgCl_2$; 1 mM DTT; protease inhibitors). After incubation on ice for 15 min the samples were centrifuged at 2.000 g for 8 min and the cell pellet was resuspended in 2xPCV of Buffer C. The cells were lysed with the help of a Dounce homogenizer (pestle B) and cell lysis was followed by light microscopy. After two centrifugation steps at 1.000 g and 4.000 g, each for 10 min, the pellet was resuspended in 3ml of Buffer D (20 mM HEPES, pH 7.9; 420 mM NaCl; 1.5 mM $MgCl_2$; 0.2 mM EDTA; 20% (v/v) Glycerol; 1 mM DTT; protease inhibitors) per 10^9 cells. After incubation at 4°C for 30 min the extract was sonicated 2 x 20 sec in a volume of 200 µl (alternatively 3x 20 sec in a volume of 250 µl) with the Bioruptor (H, Diagenode) and centrifuged at 17.000 g for 15 min. After centrifugation the nuclear fraction was collected and dialysed against Buffer D containing 300 mM NaCl.

MB III whole cell extracts were prepared according to the Manley protocol (33) and dialysed against AM100.

For immunoprecipitation experiments, extracts were incubated with anti-Flag M2 agarose in the presence of 0.02% NP-40 or 0.25% Triton X-100, protease inhibitors and DTT [1mM]. Flag-RPA116-containing complexes were additionally washed with AM300 buffer [300 mM NaCl]). Proteins were eluted with 0.25 mg/ml Flag-peptide. If needed proteins were concentrated with Strata Clean resin (Stratagene) or by TCA-precipitation. Proteins were separated by SDS-PAGE and either analyzed by Western blotting, silver- or Coomassie-staining, cut out of the gel and subjected to MALDI-TOF mass spectrometry.

Fractionation by glycerol gradient and Superose 6 gel filtration - 500 µl of MB III whole cell extract was applied on a 12 ml 10% - 45% glycerol gradient (AM100) and centrifuged with 35 K (Sw 41 Ti rotor) in a Optima-LE 80K ultracentrifuge (Beckman Coulter) at 4°C for 12 h (no break). Subsequently 500 µl fractions were collected and proteins were separated by SDS-PAGE and subjected to Western blotting.

HeLa nuclear extract was incubated with or without 10 µg/ml RNase A (Sigma) at 4 °C for 2 h prior to Superose 6 HR 10/30 (Pharmacia) fractionation. 500 µl fractions were collected and proteins were concentrated with the Strata Clean resin (Stratagene) and analyzed by Western blotting.

Antibodies - The following antibodies were used for Western blotting, ChIP and immunostaining: rabbit polyclonal α-RPA116 (30), rabbit polyclonal α-PAF53 (34), and α-TIF-IA (35) were kindly provided by I. Grummt, rabbit polyclonal α-Mybbp1a (generated to a GST-fusion protein containing amino acid residues 976-1263 of human Mybbp1a) and α-mouse Mybbp1a (23), mouse monoclonal α-Flag (M2, Sigma), rabbit polyclonal α-Flag (Sigma), mouse monoclonal α-tubulin (Dm1a, Sigma), rabbit polyclonal α-RPA194 (sc-28174, Santa Cruz Biotechnology), α-BrdU (Roche), α-Pes1 (36), α-TTF-I (37), α-Fibrillarin (P2G3, (38)), α-B23 (sc-56622, Santa Cruz Biotechnology), α-EBP2 (kindly provided by L. Frappier (39)), α-rpS2 (kindly provided by M. Bedford (40)), α-DDX21 (PTG), α-Nol1 (PTG), α-GFP-Alexa488 (GBA-488, ChromoTek), goat-α-mouse-Alexa488 $F(ab')_2$ (Molecular Probes) and goat-α-rabbit-Alexa594 (Molecular Probes).

RNA Pol I reporter assay - HeLa cells were transfected with Polyfect reagent (Qiagen) according to the manufacturer's instruction with the indicated amounts of expression construct together with empty vector DNA to adjust DNA concentration and the pHrD-IRES firefly reporter construct (kind gift of S. T. Jacob, (41)) as a reporter for RNA Pol I transcription activity. A plasmid carrying the renilla luciferase gene under the control of a TK promoter (transcribed by RNA polymerase II) was co-transfected in each experiment to normalize for differences in transfection efficiency. 48 h after transfection, luciferase activity was measured using the Dual Luciferase Assay kit (Promega). The firefly luciferase counts of the RNA polymerase I reporter constructs were divided by the Renilla luciferase counts and compared to control transfections with empty vector. Average and standard deviation values of 3 biological replicates (each in technical duplicates) are shown. Protein levels were monitored by Western blotting.

siRNA-mediated protein depletion - The day before transfection $2x10^5$ Hela cells were seeded per well (6 well format). 20 µM siRNA were transfected using Oligofectamine (Invitrogen) according to the manufacturer's instruction. The following siRNAs (Thermo or MWG) were used:

Control (Ctrl; Luciferase): 5'-CUU ACG CUG AGU ACU UCG AdTdT;

Mybbp1a.1: 5'-GCC GAC UUG AAU AUA AUA CdTdT;

Mybbp1a.2: 5'-UGG AUC AUC UUU CGA UUG GdTdT;

Mybbp1a.3: 5'-AUA CGC AAG CUG UUU CUA AdTdT;

PES1 (ORF): 5'-AGG UCU UCC UGU CCA UCA AdTdT;

TIF-IA: 5'- CAA AGG ATC TAT ATC GCG AdTdT

The three different siRNAs directed against Mybbp1a had similar effects on rRNA gene transcription and pre-rRNA processing (Fig. S3), ruling out off-target effects.

RNA extraction and quantitative real-time PCR - RNA was extracted from HeLa cells with the RNeasy kit (Qiagen) according to the manufacturer's instructions. 1 µg of total RNA was used for reverse transcription. A 20 µl reaction contained 2 µl of random primer (500 µg/ml, Promega), 2 µl of dNTPs (2.5 mM each, Bioline) and sterile water as added to a total volume of 12 µl. RNA was added and incubated for 5 min at 65°C. After cooling down the reaction was supplemented with 5x First-Strand-Buffer (Invitrogen), 2 µl 0.1 M RNase-free DTT (Invitrogen) and 1 µl RNasin (Promega) and incubated for 2 min at 37°C. 200 U of M-MLV Reverse Transcriptase (Invitrogen) were added and the reactions were incubated for 1 h at 37°C and subsequently heat-inactivated.

Quantitative PCR was carried out using the ABI PRISM 7000 Sequence detection system (Applied Biosystems). Taqman 2xPCR Master Mix (Applied Biosystems) was used according to the manufacturer's instruction. To detect 47S rRNA precursor the following oligos were used: forward +132/+149 CCT GCT GTT CTC TCG CGC, reverse +198/+181 GGT CAG AGA CCC GGA CCC and Taqman: +155/+174 AGC GTC CCG ACT CCC GGT GC. A β-actin-mRNA amplicon was used for normalization (forward: HBacF +927/+945 TGC CGA CAG GAT GCA GAA G, reverse: +1026/+1006 GCC GAT CCA CAC GGA GTA CTT and Taqman +980/+1003 TCA AGA TCA TTG CTC CTC CTG AGC). For both amplicons an annealing temperature of 60°C was applied.

Northern blot - Total RNA of transfected HeLa cells was isolated using RNeasy (Qiagen). 5 mg RNA was separated by electrophoresis on 1 % agarose-formaldehyde gel and blotted onto a Hybond N+ membrane (Amersham Biosciences). The filter was washed with 2x SSC, dried and RNA was UV cross-linked. The filter was prehybridized for 1 h at 65°C with Church buffer and hybridized for 4 h with a specific ^{32}P-labeled probe. 5'ETS probe: CGG AGG CCC AAC CTC TCC GAC GAC AGG TCG CCA GAG GAC AGC GTG TCA GC; ITS1 probe: CCT CCG CGC CGG AAC GCG CTA GGT ACC TGG ACG GCG GGG GGG CGG ACG. The DNA oligonucleotides were 5' end-labeled using T4 polynucleoltide kinase in the presence of [g-^{32}P]-ATP. After hybridization the filters were washed with three changes (30 min each) of 0.2x SSC, 0.1% SDS at 65°C. Radioactive signals were detected using a Phosphoimager and quantified using the MultiGauge software.

Polysome gradient - A total of 2 x 10^7 293-cells grown in rich medium and pre-treated with 50 µg/ml cycloheximide for 5 minutes at 37°C were harvested and washed two times with cold phosphate-buffered saline containing 50 µg/ml cycloheximide. Cells were resuspended in 600 µl polysome buffer (20 mM Tris-HCl, pH 7.5, 5 mM MgCl$_2$, 50 mM KCl, 1 mM DTT, 50 µg/ml). NP-40 was added to a final concentration of 0.3% and total cell lysates were sonified three times for 30 s. A total of 250 µg RNA was loaded onto a 10 ml 10-50% linear sucrose gradient in polysome buffer. Subsequently, sucrose gradients were centrifuged at 38 krpm for 2 h in a SW40Ti rotor. Fractions of 500 µl each were collected, while the OD$_{254}$ was measured continuously. Proteins were concentrated by TCA precipitation and analyzed by Western blot.

Chromatin immunoprecipitations - ChIP experiments were performed using rabbit polyclonal α-RPA116, rabbit polyclonal α-Mybbp1a, rabbit polyclonal α-Flag and α-TTF-I antibodies as described (5,42). Purified DNA of the immunoprecipitates and of input DNA were analysed by real-time PCR using the SYBR Green (Applied Biosystems) quantitation method according to the manufacturer's instruction on an ABI PRISM 7000 Sequence detection system (Applied Biosystems). Results were calculated relative to standard curve values, corrected for nonspecific binding (normal rabbit IgG ChIP) and presented as percentage of input DNA. The following primer sequences for the rDNA loci were used: for the promoter: forward 5'-ATG GTG GCG TTT TTG GGG and reverse 5'-AGG CGG CTC AAG GCA GGA G (product -133 to +116 relative to the transcription start site) and the intergenic spacer (IGS): forward 5'-CGC TGT CCA TCT CTG TCT TTC TAT G and reverse 5'-ATA CAC CGA GTG GGG AAG CC (product +22730 to +22906 relative to the transcription start site). In ChIP experiments shown in Fig. S3 a rabbit polyclonal α-RPA194 antibody was used and real-time quantitative PCR experiments were performed in a Rotor-Gene Q (Qiagen) instrument with the following primers and Sybr GREEN detection: Hr42857F (Promoter forward): 5' ATG GTG GCG TTT TTG GGG AC; Hr42964R (Promoter reverse): 5' CGA AAG ATA TAC CTC CCC CG; Hr5232F (18S forward): GGT AAC CCG TTG AAC CCC ATT C; Hr5375R (18S reverse): GCC TCA CTA AAC CAT CCA ATC G; Hr9661F (28S forward): 5' CGA ATG ATT AGA GGT CTT GGG GC; Hr9860R (28S reverse): 5' TGG GGT

CTG ATG AGC GTC GG; Hr36189F (IGS forward): 5' TCG CCG ACT CTC TCT TGA CTT G; Hr36399R (IGS reverse): 5' TGG AGC ACA GTG ACA CAA CTA TGG. The numbers of human rDNA (Hr) oligos indicate the position of the 5' end relative to the transcription start site (+1) in the repeat unit (GenBank Acc. No. U13369).

Immunofluorescent staining and image capture - Cells were grown on coverslips or in Labtech chambers overnight and fixed in ice-cold methanol/acetone (1:1) for 1 min. Alternatively, cells were fixed in 2% paraformaldehyde/PBS on ice for 15 min, and permeabilized with 0.25% Triton X-100 in the presence of 1% paraformaldehyde/PBS on ice for 10 min. Unspecific binding was blocked with PBS-Tween 0,01% (PBS-T) containing 2% BSA and 5% goat serum for 1 h. Primary antibodies were incubated in blocking solution at RT for 1 h, or at 4° C in a humidified chamber over night. Cells were washed with PBS-T and incubated with Cy2- or Cy3-labeled secondary antibodies (Dianova) in blocking solution at RT for 1 h. DNA was counterstained with Hoechst 33342 stain (Sigma) and mounted in Vectashield (Axxora). Fluorescence images were acquired with a Zeiss Axiovert 200 inverse microscope.

To assess RNA-dependent localization of proteins, HeLa cells were washed with PBS and incubated with PBS containing 0.1% (v/v) Triton X-100 for 10 min and subsequently incubated with 1 mg/ml RNase A (Sigma) in PBS at RT for 20 min. Control cells were incubated with either 3 µl/ml RNase-free DNase I (Roche) and 3 mM $MgCl_2$ or both, RNase A and DNase I. Cells were washed with PBS, fixed and prepared for immunofluorescence microscopy as described above.

HeLa cells were incubated in DMEM containing 10 µM BrdU at 37°C for 30 min, washed with PBS-T and fixed with 4% formaldehyde/PBS at RT for 10 min. Cells were washed, permeabilized with 0.2% Triton X-100/PBS and incubated with 2N HCl/PBS for 10 min. After two washing steps cells were analysed by immunostaining for the presence of BrdU incorporation.

Super-resolution fluorescence microscopy - HeLa cells were grown on coverslips and transfected with EGFP-RPA43 (43). Non-transfected and transfected cells were fixed with 4% paraformaldehyde in 1xPBS for 10 minutes, permeabilized with 1% Triton X-100 in 1xPBS for 10 minutes and immunofluorescence detections of Mybbp1a, fibrillarin, B23/nucleophosmin and GFP-RPA43 were performed. The nuclei were counterstained with DAPI. Super-resolution fluorescence microscopy was performed with a DeltaVision OMX V3 3D-SIM system (Applied Precision) equipped with a 100x/1.40 NA PlanApo oil immersion objective (Olympus), Cascade II:512 EMCCD cameras (Photometrics) and 405, 488 and 593 nm diode lasers. Image stacks of 8-10 µm were recorded with a z-distances of 125 nm. Iterative 3D deconvolution, SI reconstruction and image processing was performed with the SoftWoRx 3.7 imaging software package (Applied Precision).

RESULTS

RNA Polymerase I is associated with Mybbp1a - To reveal potential regulators that act at the level of transcription initiation and elongation, we generated a murine MB III cell line stably expressing Flag-tagged RPA116 (Flag-RPA116-MBIII), the second-largest subunit of RNA Pol I (30). The N-terminally tagged protein was constitutively expressed at low levels in this cell line and localised similarly to the endogenous protein (Fig. 1A). Flag-RPA116 was fully incorporated into the RNA Pol I complex, as revealed by co-immunoprecipitation analysis. Flag-RPA116 co-purified with PAF53, a known subunit of the RNA Pol I complex (Fig. 1B).

Whole cell extracts were prepared from MB III and Flag-RPA116-MB III cells growing in suspension. Immunoaffinity purifications were performed under conditions that preserve complex integrity and generate transcriptionally active RNA Pol I complexes (Fig. S1). The purified proteins were subjected to protein gel electrophoresis and subsequent mass spectrometric analysis (data not shown). Mybbp1a (accession number NP_058056) was identified as an RNA Pol I interacting protein by MALDI-TOF analysis. The specific association of Mybbp1a and RNA Pol I was verified by co-immunoprecipitation experiments and western blot analysis (Fig. 1C).

Mybbp1a was originally identified as an interacting partner of the c-myb proto-oncogene product in mouse cell lines. In certain cell lines, a specific portion of mouse Mybbp1a (mMybbp1a) is processed by proteolytic cleavage to generate the N-terminal fragment $p67^{MBP}$ (23). The existence of such post-translational cleavage products has also been confirmed in human cell lines. After exposing HeLa cells to UV light or chemicals that impair transcription, Ishii and colleagues observed the appearance of N-terminal fragments of Mybbp1a with molecular weights of 67 kDa and 140 kDa (p67^{MBP} and p140^{MBP}, respectively) as well a translocation of the full-length protein and its cleavage products from the nucleolus to the nucleoplasm (44)(Fig. 1D).

Next, we verified the potential Mybbp1a/RNA Pol I association in human HeLa cells by studying protein localisation. In agreement with previous observations (44,45), Mybbp1a preferentially localises to the nucleolus also in HeLa cells as shown by immunofluorescence experiments that detect the endogenous human protein and transiently transfected mouse and human Flag-Mybbp1a protein (Fig. 1E). In order to reveal the subnucleolar distribution of Mybbp1a, the protein was visualized at subdiffraction resolution in parallel with marker proteins of the different functional regions of the nucleolus. The RNA Pol I subunit RPA43, fibrillarin and B23/nucleophosmin served as markers for the fibrillar centre, dense fibrillar component and granular component, respectively. The pictures reveal that Mybbp1a localizes closer to, or overlaps in part with RNA Pol I and fibrillarin, but not with B23/nucleophosmin suggesting a role in transcription and early processing (Fig. 1F). Mybbp1a was shown to shuttle between the nucleus and the cytoplasma and in agreement with these studies, we detected different levels of Mybbp1a in these compartments (24,44).

Mybbp1a represses rRNA gene transcription - The subnucleolar distribution of Mybbp1a, its interaction with RNA Pol I and the fact that the protein is widely conserved throughout evolution, orthologs have been identified in animals, plants and fungi (23,31,46) suggest that Mybbp1a may play a role in the regulation of rRNA synthesis. First, the physical association of Mybbp1a with the RNA Pol I complex was confirmed by co-immunoprecipitation experiments using the transiently transfected Flag-Mybbp1a construct. Affinity tag purification revealed the specific interaction of Mybbp1a with PAF53, a subunit of the RNA Pol I complex (Fig. 2A). Snf2h has been previously described as an interacting protein of Mybbp1a and was used as a positive control (47). Next we tested Mybbp1a function in the regulation of rRNA gene transcription, using a reporter system in HeLa cells. To visualise RNA Pol I activity, we employed the human rRNA minigene construct pHrD-Ires-Luc that harbours the rRNA gene promoter (-410 bp to +314 bp relative to the transcription start site) followed by an internal ribosome entry site (IRES) and the coding sequence for the firefly luciferase protein (Fig. 2B) (41,48). The IRES sequence allows translation of the rRNA Pol I transcripts and relative quantification of the minigene RNA levels via the luciferase activity. RNA Pol I transcription efficiency from the minigene construct was normalised to a co-transfected RNA Pol II-dependent construct expressing the Renilla luciferase (Fig. 2B).

Overexpression of human or mouse Mybbp1a in HeLa cells resulted in a dose-dependent transcriptional repression of the rRNA minigene expression, comparable to the repressive effect of Tip5 (Figs. 2C and S2), which is the large subunit of the nucleolar remodelling complex, NoRC, that serves to silence rRNA genes by changing their chromatin structure and initiating heterochromatinisation of rDNA (32,49,50). In contrast, overexpression of equal amounts of a C-terminally truncated form of mouse Mybbp1a (mp67^{MBP}*NLS), containing the SV40-T-antigen NLS to target the protein to the nucleus and nucleolus (24)(Fig. 1D), had no effect on RNA Pol I-dependent transcription (Fig. 2C). These results suggest that the C-terminus of Mybbp1a is required for efficient transcriptional repression. To obtain more insight into the action of Mybbp1a at rRNA genes ChIP experiments were performed. Nuclear and nucleolar extracts of control cells and cells overexpressing the Flag-tagged Mybbp1a were immunoprecipitated with antibodies against the Flag-tag, hMybbp1a, RPA194, RPA116 and TTF-I (Figs. 2D and S3). In these experiments neither the α-Flag, nor the α-Mybbp1a antibodies were able to co-precipitate rDNA fragments, which suggests that Mybbp1a functions at a distance that cannot be captured by formaldehyde crosslink. However, we did observe reduced rDNA binding of RNA Pol I and TTF-I upon overexpression of Flag-Mybbp1a, correlating with Mybbp1a dependent Pol I transcription repression. The results suggest that Mybbp1a may repress transcription through its binding to the RNA Pol I complex.

Mybbp1a is involved in pre-rRNA processing - In a recent study, Greenblatt and colleagues analysed the composition of yeast rRNA-processing complexes and found that Pol5p, the suggested yeast homolog of Mybbp1a, is associated with the UtpA complex (51). UtpA is the possible equivalent of the t-Utp sub-complex of the SSU processome that was identified in an independent study (2). Accordingly, we studied the role of Mybbp1a in pre-rRNA processing, which involves a number of ordered and consecutive endo- and exonucleolytic cleavages of the 47S precursor to produce the 18S, 5.8S and 28S rRNAs. A short overview of the major mammalian rRNA processing pathways is depicted in Fig. 3A (for a detailed review see (52)).

The reporter assay described above allowed the uncoupling of rRNA transcription from processing, whereas the analysis of cellular rRNA levels reflects the sum of these processes. To characterize gain-of-function effects of Mybbp1a, 47S precursor, intermediate and mature rRNA levels were measured in qRT-PCR and Northern blot experiments (Figs. 3). To our surprise, overexpression of Mybbp1a resulted in elevated steady-state levels of the 5' external transcribed spacer (5'ETS) fragment of rRNA when measured by qRT-PCR (Fig. 3B).

This result did apparently contradict the reporter assay that monitors only transcription initiation (Fig. 2C). In order to confirm the qRT-PCR in an independent assay and to rule out the possible accumulation of the 5'ETS fragment after co-transcriptional cleavage, 47S pre-rRNA levels were measured by the Northern blot assay (Fig. 3C, upper panel). Since the result confirmed the qRT-PCR observations, we hypothesize a dominant negative effect of Mybbp1a on pre-rRNA processing. The difference between both assays is that the reporter assay using the core promoter is only capable to reveal effects on transcription initiation, whereas qRT-PCR and Northern blot analyze the combined effects of transcription initiation and pre-rRNA processing. An inhibition of rRNA processing steps may result in 47/45S rRNA accumulation even though rRNA transcription levels are decreased. Thus, we investigated the levels of rRNA processing intermediates by Northern blot analysis of the RNA (Fig. 3C). The quantification of the data (Fig. 3D) approved our hypothesis, demonstrating accumulation of the 47/45S, 41S and to a lower level of 30S and 21S rRNA intermediates. Mainly pathway A (Fig. 3A) was affected by overexpression of Mybbp1a, however also minor effects on the pathway B were observed. Our data suggests that Mybbp1a participates in transcriptional repression and is involved in pre-rRNA processing.

Mybbp1a associates with the ribosome biogenesis machinery - Several large RNA-containing complexes are involved in ribosome synthesis and implement pre-rRNA processing and pre-ribosome assembly in accordance with rDNA transcription (reviewed in (53)). In order to reveal the binding of Mybbp1a to RNA-containing complexes we first monitored the cellular localisation of Mybbp1a after RNase A treatment in HeLa cells (Fig. S4). Immunodetection of the endogenous protein revealed a relocalisation of Mybbp1a from the nucleoli to the nucleoplasm upon RNase A treatment, whereas the Pol I-specific and rDNA-binding Transcription Termination Factor-I (TTF-I) remained nucleolar. Further, control treatment with DNaseI, an enzyme that does not hydrolyse RNA, did not change the localisation of Mybbp1a. These findings suggest that nucleolar localisation of Mybbp1a depends on the interaction with a nucleolar RNA component and confirm very recent data obtained in the human breast cancer cell line MCF-7 (54).

We next investigated whether Mybbp1a is part of an RNA-containing complex, as suggested by the immunofluorescence experiments. Therefore, HeLa nuclear extract was fractionated by gel filtration on a Superose 6 column, and the fractions were assayed for the presence of Mybbp1a (Fig. 4A). Mybbp1a mostly eluted with an apparent molecular mass in the MDa range, co-migrating with the RNA Pol I holoenzyme complex. In agreement with this observation, a recent analysis of the protein composition of transcription factories also revealed the association of Mybbp1a with the RNA Pol I transcription factory (55). Furthermore, the protein co-migrates with fibrillarin, a protein involved in several steps of ribosome biogenesis (56). Mybbp1a, and in part fibrillarin, were shifted to fractions corresponding to lower molecular masses when the extract was incubated with RNase A, confirming that it is part of a large multi-subunit RNase-sensitive complex such as the ribosome biosynthesis machinery. To confirm that fibrillarin and Mybbp1a are present in a single complex, we transfected HeLa cells with the human Flag-Mybbp1a expression construct and performed co-immunoprecipitation experiments. Flag-Mybbp1a co-precipitated fibrillarin, and fibrillarin also specifically eluted with Mybbp1a from the affinity matrix (Fig. 4B). Our data confirm the proteomics data and identify Mybbp1a as an interactor of fibrillarin (57).

Next we studied the association of Mybbp1a with the ribosomal biogenesis machinery. We studied its sedimentation behaviour on a sucrose gradient with regard to pre-ribosomal particles and polyribosomes. Sucrose gradient centrifugation in combination with UV-profiling and Western blotting clearly revealed a co-migration of Mybbp1a with the 40- and 60S pre-ribosomal particles, whereas no Mybbp1a was detected in the mRNA-associated polysome fractions (Fig. 4C). Pes1, a factor involved in the processing of the 32S precursor, showed a preference for the 60S pre-ribosomal particle as expected. This finding suggests that Mybbp1a is involved in the maturation of the ribosomal subunits but it does not interact with the mature, translating ribosomal particles.

To reveal additional binding partners of Mybbp1a, the Flag-tagged protein was transiently transfected into HeLa cells, and associated proteins were purified by affinity chromatography, separated by gel electrophoresis and analysed by MALDI-TOF mass spectrometry (Fig. 4D). As suggested by our experiments, Mybbp1a interacts with proteins belonging to the ribosome biogenesis pathway and the small and large ribosomal proteins that are assembled during rRNA transcription. We tested several of those proteins for co-migration with Mybbp1a in the presence or absence of RNA. Interestingly, those proteins co-migrated with Mybbp1a in the large complex and were converted to distinct smaller complexes after RNase A treatment (Fig. S5).

Mybbp1a is essential for cellular proliferation - To study the consequence of Mybbp1a-dependent perturbation of ribosome biogenesis on cell proliferation, loss of function experiments were performed, using short interfering RNAs (siRNA). Knock down experiments were performed with GL3- (a control siRNA directed against the luciferase gene), TIF-IA- and Mybbp1a-specific siRNAs (Figs. 5A and S6). Knock down of Mybbp1a and TIF-IA was monitored at the protein level and followed for up to twelve days (Fig. 5A). siRNA-mediated knock down of Mybbp1a efficiently reduced protein levels from day 2 through day 7, followed by partial (day 9) and full (day 12) recovery of Mybbp1a protein levels. siRNA-mediated knock down of TIF-IA was not as efficient as Mybbp1a depletion, but a visible reduction in the protein level was detected from day 2 to day 7.

To monitor the effect of protein depletion on rRNA levels, we measured first the steady state levels of the 5' ETS by quantitative real time PCR (Fig. S6). Total cellular RNA was isolated and reverse transcribed, and the level of the 5'ETS was quantified and normalised to β-actin mRNA. In agreement with the rRNA minigene expression studies (Fig. 2), depletion of Mybbp1a resulted in an increase in pre-rRNA levels in the cell. As expected, reduced TIF-IA levels resulted in a strong decrease of pre-rRNA synthesis, as this protein is an essential transcription initiation factor (58,59) (Fig. S6).

In addition, we observed that cells depleted of either TIF-IA or Mybbp1a behaved similar and ceased cellular proliferation. BrdU-labelling experiments of Mybbp1a-depleted cells showed a reduced number of cells in S-phase (Fig. S7A). Quantification of cellular proliferation by counting cells after protein knock down (Fig. 5B) revealed a stronger effect of Mybbp1a on cellular proliferation, as compared to TIF-IA. Halted cellular proliferation correlates with the time frame of reduced protein levels (Fig. 5). According to our observation that depletion of Mybbp1a resulted in the accumulation of pre-rRNA, we would have expected increased proliferation rates after Mybbp1a knock down. These findings appear to be counterintuitive as high rDNA transcription activity and rRNA levels are the major determinants of cellular growth and proliferation, but can be explained by our experimental data on rRNA processing that indicate additional roles for Mybbp1a in growth-related processes other than rDNA transcription. Furthermore, visual inspection of the Mybbp1a knock down cells revealed an abnormal, flattened and enlarged morphology (Fig. S7B).

DISCUSSION

We identified Mybbp1a association with RNA Pol I and demonstrated that Mybbp1a serves both as a negative regulator of rRNA gene transcription and as a functional part of the ribosome biogenesis machinery. The results of the loss-of-function studies together with the gain-of-function experiments suggest that Mybbp1a plays a dual role in rRNA metabolism: first, regulating transcription initiation and second, being essential for the correct processing of the pre-rRNA. Depletion of the protein leads to a dominant anti-repression effect on rRNA synthesis, while the overexpression of Mybbp1a impairs dominantly the rRNA processing. Although ribosome biogenesis is a major determinant of cellular growth and proliferation, additional functions of Mybbp1a in growth-related processes may explain its effects on cellular proliferation. Yet, our data showed that Mybbp1a plays a role in the regulation of rRNA transcription and is an essential component of the ribosome biogenesis machinery at the same time, placing the protein at the interface of transcription and processing.

Intriguingly, Mybbp1a was very recently identified to activate the tumour suppressor p53 as a consequence of nucleolar stress (54). Upon inhibition of rRNA synthesis by TIF-IA knock down or treatment with low doses of Actinomycin D, Mybbp1a translocated to the nucleoplasm and increased the acetylation levels of p53. Mybbp1a did stimulate the interaction of p53 with the histone acetyltransferase p300 leading to the p53-dependent gene activation. Taken together, it seems that Mybbp1a plays an important role as a central regulator of proliferation, cell cycle progression and differentiation in the mammalian system. As shown by our study, Mybbp1a affects simultaneously the Pol II and Pol I transcription systems to achieve its regulatory function.

In budding and baker's yeast, the protein Pol5p was identified as the potential homolog of Mybbp1a and was shown to bind to the rRNA gene repeat (60,61). In yeast, Pol5p has been connected with an essential role in rRNA synthesis. We present here substantial evidence for the role of its potential mammalian homologue both in rRNA synthesis and processing. In the absence of Mybbp1a, rRNA synthesis became de-repressed, but cells ceased proliferation at the same time (Fig. 5 and S6). These results argue that Mybbp1a has a pro-proliferative role, as was observed in yeast. In the case of transcriptional regulation the further analysis of Mybbp1a's interaction with RNA Pol I could provide more mechanistic insights into the function of the protein. Here, the identification and function of the RNA component(s) involved in Mybbp1a-dependent regulation of rRNA synthesis would be particularly interesting. The RNase A sensitivity of the major fraction of RNA Pol I – Mybbp1a-containing complexes (Fig. 4A) suggests that the association of the proteins may takes place in a transcriptionally engaged ternary protein-DNA-RNA complex.

We propose that the accumulation of 47S pre-rRNA upon Mybbp1a depletion is a combined consequence of transcription up-regulation due to de-repression of the rRNA gene and a defect in rRNA processing. A similar effect was suggested for Pwp2 (Utp1), a component of the SSU processome (62). Depletion of Pwp2 leads to pre-rRNA accumulation due to stalling rRNA processing. In turn, when cells were overloaded with Mybbp1a, the excess of the protein may perturb dominantly the rRNA processing pathway (Fig. 3). In conclusion, it is likely that the functional role of Mybbp1a involves the coordination of transcription and processing. However, additional experiments have to be performed to unravel the detailed mechanism. These include the dissection of direct and indirect Mybbp1a effects on rDNA transcription by identifying the protein domains and/or RNA that are involved in Mybbp1a – RNA Pol I and Mybbp1a – processome interactions. Functional characterization of specific interaction-defective mutants will give insights into the molecular mechanisms of Mybbp1a-dependent regulation of ribosome biogenesis.

To initially characterize Mybbp1a's mode of action we have purified Mybbp1a-containing complexes (Fig. 4D). We identified a large variety of ribosomal proteins of both the SSU and LSU, as well as of several other factors such as Fibrillarin, DDX21, Rrs1, Ebp2 and Nol1 (yeast Nop2), to which roles in rRNA processing and ribosome assembly have been assigned in previous studies (56,63-66). This result was supported by the observation that Mybbp1a co-migrated with the SSU and LSU pre-ribosomal particles on a polysome sucrose gradient (Fig. 4C). The data show that Mybbp1a is a component of pre-ribosomal complexes and together with the effects in de-regulation pathways A + B (Fig. 3A) in pre-rRNA processing suggests that it is functionally and structurally involved in this process.

Recently, Yamauchi and co-workers have shown that Mybbp1a is processed upon ribosomal stress induction (44). Treatment of cells with actinomycin D, cisplatin or UV, all of which inhibit ribosome biogenesis, lead to proteolytical cleavage of Mybbp1a into C-terminally truncated $p140^{MBP}$ and $p67^{MBP}$ proteins. Proteolysis of Mybbp1a results in its translocation to the nucleoplasm (24,44). The full-length Mybbp1a and the processed forms were found in distinct complexes, both of which contained nucleophosmin and nucleolin, and the large complex containing the full-length protein also contained nucleostemin and ribosomal proteins (44). We speculate that the Mybbp1a-containing ribosome assembly/processing machinery identified in this study is likely to be equivalent to the large complex purified by Yamauchi and colleagues. Indeed, a recent characterisation of Mybbp1a-containing complexes in MCF-7 cells by Yanagisawa and colleagues also revealed some of the factors identified in this study, such as EBP2 and Nol1 (54), confirming our results.

Interestingly, depletion of Rrs1 or Ebp2, factors that co-purified with Mybbp1a, were also shown to affect rRNA processing, mirroring the effects observed for Mybbp1a (63,64). Rrs1 is a ribosome assembly factor that recruits the 5S rRNA and the ribosomal proteins rpL5 and rpL11 into nascent ribosomes (67). Moreover, Rrs1 seems to be involved in rDNA transcription regulation, as a yeast *rrs1* mutant has been shown to reduce transcriptional repression of the rRNA gene (63). Both Rrs1 and Ebp2 have recently been connected to a role in the progression of mitosis, as well. Mybbp1a is phosphorylated by the mitotic kinase Aurora B, and it has been revealed that depletion of Mybbp1a or Rrs1 leads to a mitotic delay and abnormalities in spindle organisation (45,68). Additionally, the involvement of Mybbp1a, rpL5, and rpL11 was shown in p53 acetylation and accumulation, which is dependent on the release of Mybbp1a from nucleolar RNA upon stress (54). This study strongly suggests a role for Mybbp1a in rRNA metabolism, based on its binding to nucleolar RNA.

We have shown that Mybbp1a is required for cellular proliferation, an effect that may relate either to its role in pre-rRNA processing or in the regulation of extra-nucleolar interaction partners. Our experiments cannot discriminate between these scenarios. Mybbp1a-depleted cells exhibit a flattened and enlarged morphology that is clearly visible on day 4 after siRNA-mediated knock down (Fig. S7B). This phenotype mirrors the 'flat cell phenotype' of Retinoblastoma (Rb)-negative SAOS-2 sarcoma cells, when overexpression of Rb leads to a cell cycle arrest in late G_1 phase (69). Thus, it would be interesting to address the possible role of Mybbp1a in coordinating ribosome biogenesis and cell cycle progression in future studies.

As transcription of rRNA genes and subsequent pre-RNA processing and ribosome assembly processes are the major energy-consuming processes in the cell, the rate of biogenesis is tightly linked to cellular proliferation. We suggest that in proliferating cells, Mybbp1a is mainly associated with the pre-ribosomal complexes where it acts as a scaffold for rRNA processing and assembly factors and is functionally required to drive efficient ribosome biogenesis. Reduced levels of ribosome biogenesis upon stress signals and/or reduced demands of ribosomes potentially result in the disassembly of pre-ribosomal particles and a translocation of Mybbp1a to the nucleoplasm. While nucleolar Mybbp1a would repress RNA Pol I transcription, the nuclear proteins would modulate the activity of transcription regulators, such as c-myb, PGC-1α, NF-κB or p53, to cease cell cycle progression, proliferation and energy production.

REFERENCES

1. Warner, J. R. (1999) *Trends Biochem Sci* **24**(11), 437-440
2. Gallagher, J. E., Dunbar, D. A., Granneman, S., Mitchell, B. M., Osheim, Y., Beyer, A. L., and Baserga, S. J. (2004) *Genes Dev* **18**(20), 2506-2517
3. Schneider, D. A., Michel, A., Sikes, M. L., Vu, L., Dodd, J. A., Salgia, S., Osheim, Y. N., Beyer, A. L., and Nomura, M. (2007) *Mol Cell* **26**(2), 217-229
4. Grummt, I., and Pikaard, C. S. (2003) *Nat Rev Mol Cell Biol* **4**(8), 641-649
5. Nemeth, A., Guibert, S., Tiwari, V. K., Ohlsson, R., and Langst, G. (2008) *EMBO J* **27**(8), 1255-1265
6. Nemeth, A., and Langst, G. (2008) *Epigenetics : official journal of the DNA Methylation Society* **3**(5), 243-245
7. Nemeth, A., and Langst, G. (2011) *Trends Genet* **27**(4), 149-156
8. Mayer, C., Zhao, J., Yuan, X., and Grummt, I. (2004) *Genes Dev* **18**(4), 423-434
9. Hannan, K. M., Brandenburger, Y., Jenkins, A., Sharkey, K., Cavanaugh, A., Rothblum, L., Moss, T., Poortinga, G., McArthur, G. A., Pearson, R. B., and Hannan, R. D. (2003) *Mol Cell Biol* **23**(23), 8862-8877
10. Zhao, J., Yuan, X., Frodin, M., and Grummt, I. (2003) *Mol Cell* **11**(2), 405-413
11. Stefanovsky, V. Y., Pelletier, G., Hannan, R., Gagnon-Kugler, T., Rothblum, L. I., and Moss, T. (2001) *Mol Cell* **8**(5), 1063-1073
12. Dragon, F., Gallagher, J. E., Compagnone-Post, P. A., Mitchell, B. M., Porwancher, K. A., Wehner, K. A., Wormsley, S., Settlage, R. E., Shabanowitz, J., Osheim, Y., Beyer, A. L., Hunt, D. F., and Baserga, S. J. (2002) *Nature* **417**(6892), 967-970
13. Osheim, Y. N., French, S. L., Keck, K. M., Champion, E. A., Spasov, K., Dragon, F., Baserga, S. J., and Beyer, A. L. (2004) *Mol Cell* **16**(6), 943-954
14. Mougey, E. B., O'Reilly, M., Osheim, Y., Miller, O. L., Jr., Beyer, A., and Sollner-Webb, B. (1993) *Genes Dev* **7**(8), 1609-1619
15. Kos, M., and Tollervey, D. (2010) *Mol Cell* **37**(6), 809-820
16. Prieto, J. L., and McStay, B. (2007) *Genes Dev* **21**(16), 2041-2054

17. Stefanovsky, V., Langlois, F., Gagnon-Kugler, T., Rothblum, L. I., and Moss, T. (2006) *Mol Cell* **21**(5), 629-639
18. Schneider, D. A., French, S. L., Osheim, Y. N., Bailey, A. O., Vu, L., Dodd, J., Yates, J. R., Beyer, A. L., and Nomura, M. (2006) *Proc Natl Acad Sci U S A* **103**(34), 12707-12712
19. Grummt, I. (2003) *Genes Dev* **17**(14), 1691-1702
20. Milkereit, P., Gadal, O., Podtelejnikov, A., Trumtel, S., Gas, N., Petfalski, E., Tollervey, D., Mann, M., Hurt, E., and Tschochner, H. (2001) *Cell* **105**(4), 499-509
21. Ferreira-Cerca, S., Poll, G., Kuhn, H., Neueder, A., Jakob, S., Tschochner, H., and Milkereit, P. (2007) *Mol Cell* **28**(3), 446-457
22. Holmstrom, T. H., Mialon, A., Kallio, M., Nymalm, Y., Mannermaa, L., Holm, T., Johansson, H., Black, E., Gillespie, D., Salminen, T. A., Langel, U., Valdez, B. C., and Westermarck, J. (2008) *J Biol Chem* **283**(11), 7046-7053
23. Tavner, F. J., Simpson, R., Tashiro, S., Favier, D., Jenkins, N. A., Gilbert, D. J., Copeland, N. G., Macmillan, E. M., Lutwyche, J., Keough, R. A., Ishii, S., and Gonda, T. J. (1998) *Mol Cell Biol* **18**(2), 989-1002
24. Keough, R. A., Macmillan, E. M., Lutwyche, J. K., Gardner, J. M., Tavner, F. J., Jans, D. A., Henderson, B. R., and Gonda, T. J. (2003) *Exp Cell Res* **289**(1), 108-123
25. Fan, M., Rhee, J., St-Pierre, J., Handschin, C., Puigserver, P., Lin, J., Jaeger, S., Erdjument-Bromage, H., Tempst, P., and Spiegelman, B. M. (2004) *Genes Dev* **18**(3), 278-289
26. Diaz, V. M., Mori, S., Longobardi, E., Menendez, G., Ferrai, C., Keough, R. A., Bachi, A., and Blasi, F. (2007) *Mol Cell Biol* **27**(22), 7981-7990
27. Owen, H. R., Elser, M., Cheung, E., Gersbach, M., Kraus, W. L., and Hottiger, M. O. (2007) *J Mol Biol* **366**(3), 725-736
28. Jones, L. C., Okino, S. T., Gonda, T. J., and Whitlock, J. P., Jr. (2002) *J Biol Chem* **277**(25), 22515-22519
29. Hara, Y., Onishi, Y., Oishi, K., Miyazaki, K., Fukamizu, A., and Ishida, N. (2009) *Nucleic Acids Res* **37**(4), 1115-1126
30. Seither, P., and Grummt, I. (1996) *Genomics* **37**(1), 135-139
31. Keough, R., Woollatt, E., Crawford, J., Sutherland, G. R., Plummer, S., Casey, G., and Gonda, T. J. (1999) *Genomics* **62**(3), 483-489
32. Strohner, R., Nemeth, A., Jansa, P., Hofmann-Rohrer, U., Santoro, R., Langst, G., and Grummt, I. (2001) *EMBO J* **20**(17), 4892-4900
33. Manley, J. L., Fire, A., Cano, A., Sharp, P. A., and Gefter, M. L. (1980) *Proc Natl Acad Sci U S A* **77**(7), 3855-3859
34. Seither, P., Zatsepina, O., Hoffmann, M., and Grummt, I. (1997) *Chromosoma* **106**(4), 216-225
35. Bodem, J., Dobreva, G., Hoffmann-Rohrer, U., Iben, S., Zentgraf, H., Delius, H., Vingron, M., and Grummt, I. (2000) *EMBO Rep* **1**(2), 171-175
36. Holzel, M., Rohrmoser, M., Schlee, M., Grimm, T., Harasim, T., Malamoussi, A., Gruber-Eber, A., Kremmer, E., Hiddemann, W., Bornkamm, G. W., and Eick, D. (2005) *J Cell Biol* **170**(3), 367-378
37. Evers, R., Smid, A., Rudloff, U., Lottspeich, F., and Grummt, I. (1995) *EMBO J* **14**(6), 1248-1256
38. Christensen, M. E., and Banker, N. (1992) *Cell Biol Int Rep* **16**(11), 1119-1131
39. Wu, H., Ceccarelli, D. F., and Frappier, L. (2000) *EMBO Rep* **1**(2), 140-144
40. Swiercz, R., Person, M. D., and Bedford, M. T. (2005) *Biochem J* **386**(Pt 1), 85-91
41. Ghoshal, K., Majumder, S., Datta, J., Motiwala, T., Bai, S., Sharma, S. M., Frankel, W., and Jacob, S. T. (2004) *J Biol Chem* **279**(8), 6783-6793
42. O'Sullivan, A. C., Sullivan, G. J., and McStay, B. (2002) *Mol Cell Biol* **22**(2), 657-668
43. Dundr, M., Hoffmann-Rohrer, U., Hu, Q., Grummt, I., Rothblum, L. I., Phair, R. D., and Misteli, T. (2002) *Science* **298**(5598), 1623-1626
44. Yamauchi, T., Keough, R. A., Gonda, T. J., and Ishii, S. (2008) *Genes Cells* **13**(1), 27-39
45. Perrera, C., Colombo, R., Valsasina, B., Carpinelli, P., Troiani, S., Modugno, M., Gianellini, L., Cappella, P., Isacchi, A., Moll, J., and Rusconi, L. (2010) *J Biol Chem*
46. Yang, W., Rogozin, I. B., and Koonin, E. V. (2003) *Cell Cycle* **2**(2), 120-122
47. Cavellan, E., Asp, P., Percipalle, P., and Farrants, A. K. (2006) *J Biol Chem* **281**(24), 16264-16271

48. Nemeth, A., Strohner, R., Grummt, I., and Langst, G. (2004) *Nucleic Acids Res* **32**(14), 4091-4099
49. Santoro, R., Li, J., and Grummt, I. (2002) *Nat Genet* **32**(3), 393-396
50. Li, J., Langst, G., and Grummt, I. (2006) *EMBO J* **25**(24), 5735-5741
51. Krogan, N. J., Peng, W. T., Cagney, G., Robinson, M. D., Haw, R., Zhong, G., Guo, X., Zhang, X., Canadien, V., Richards, D. P., Beattie, B. K., Lalev, A., Zhang, W., Davierwala, A. P., Mnaimneh, S., Starostine, A., Tikuisis, A. P., Grigull, J., Datta, N., Bray, J. E., Hughes, T. R., Emili, A., and Greenblatt, J. F. (2004) *Mol Cell* **13**(2), 225-239
52. Henras, A. K., Soudet, J., Gerus, M., Lebaron, S., Caizergues-Ferrer, M., Mougin, A., and Henry, Y. (2008) *Cell Mol Life Sci* **65**(15), 2334-2359
53. Granneman, S., and Baserga, S. J. (2005) *Curr Opin Cell Biol* **17**(3), 281-286
54. Kuroda, T., Murayama, A., Katagiri, N., Ohta, Y. M., Fujita, E., Masumoto, H., Ema, M., Takahashi, S., Kimura, K., and Yanagisawa, J. (2011) *EMBO J* **30**(6), 1054-1066
55. Melnik, S., Deng, B., Papantonis, A., Baboo, S., Carr, I. M., and Cook, P. R. (2011) *Nat Methods* **8**(11), 963-968
56. Tollervey, D., Lehtonen, H., Jansen, R., Kern, H., and Hurt, E. C. (1993) *Cell* **72**(3), 443-457
57. Yanagida, M., Hayano, T., Yamauchi, Y., Shinkawa, T., Natsume, T., Isobe, T., and Takahashi, N. (2004) *J Biol Chem* **279**(3), 1607-1614
58. Buttgereit, D., Pflugfelder, G., and Grummt, I. (1985) *Nucleic Acids Res* **13**(22), 8165-8180
59. Schnapp, A., Pfleiderer, C., Rosenbauer, H., and Grummt, I. (1990) *EMBO J* **9**(9), 2857-2863
60. Nadeem, F. K., Blair, D., and McInerny, C. J. (2006) *Mol Genet Genomics* **276**(4), 391-401
61. Shimizu, K., Kawasaki, Y., Hiraga, S., Tawaramoto, M., Nakashima, N., and Sugino, A. (2002) *Proc Natl Acad Sci U S A* **99**(14), 9133-9138
62. Bernstein, K. A., Bleichert, F., Bean, J. M., Cross, F. R., and Baserga, S. J. (2007) *Mol Biol Cell* **18**(3), 953-964
63. Tsuno, A., Miyoshi, K., Tsujii, R., Miyakawa, T., and Mizuta, K. (2000) *Mol Cell Biol* **20**(6), 2066-2074
64. Tsujii, R., Miyoshi, K., Tsuno, A., Matsui, Y., Toh-e, A., Miyakawa, T., and Mizuta, K. (2000) *Genes Cells* **5**(7), 543-553
65. Hong, B., Brockenbrough, J. S., Wu, P., and Aris, J. P. (1997) *Mol Cell Biol* **17**(1), 378-388
66. Henning, D., So, R. B., Jin, R., Lau, L. F., and Valdez, B. C. (2003) *J Biol Chem* **278**(52), 52307-52314
67. Zhang, J., Harnpicharnchai, P., Jakovljevic, J., Tang, L., Guo, Y., Oeffinger, M., Rout, M. P., Hiley, S. L., Hughes, T., and Woolford, J. L., Jr. (2007) *Genes Dev* **21**(20), 2580-2592
68. Gambe, A. E., Matsunaga, S., Takata, H., Ono-Maniwa, R., Baba, A., Uchiyama, S., and Fukui, K. (2009) *FEBS Lett* **583**(12), 1951-1956
69. Hinds, P. W., Mittnacht, S., Dulic, V., Arnold, A., Reed, S. I., and Weinberg, R. A. (1992) *Cell* **70**(6), 993-1006
70. Marchler-Bauer, A., Anderson, J. B., Chitsaz, F., Derbyshire, M. K., DeWeese-Scott, C., Fong, J. H., Geer, L. Y., Geer, R. C., Gonzales, N. R., Gwadz, M., He, S., Hurwitz, D. I., Jackson, J. D., Ke, Z., Lanczycki, C. J., Liebert, C. A., Liu, C., Lu, F., Lu, S., Marchler, G. H., Mullokandov, M., Song, J. S., Tasneem, A., Thanki, N., Yamashita, R. A., Zhang, D., Zhang, N., and Bryant, S. H. (2009) *Nucleic Acids Res* **37**(Database issue), D205-210
71. Schermelleh, L., Carlton, P. M., Haase, S., Shao, L., Winoto, L., Kner, P., Burke, B., Cardoso, M. C., Agard, D. A., Gustafsson, M. G., Leonhardt, H., and Sedat, J. W. (2008) *Science* **320**(5881), 1332-1336

Acknowledgments - We thank R. Strohner, A. Brehm, A. Hochheimer and T. Straub for stimulating and helpful discussions and A. Maiser for technical assistance. We are very thankful to K. Dachauer for technical help. We thank I. Grummt for the generous gifts of antibodies and cDNA construct and T. Misteli for the GFP-RPA43 plasmid.

FOOTNOTES

*This work was supported by DFG grants to GL, DE, AI and HL and the Bayerisches Genomforschungsnetzwerk (BayGene) to GL.

[1] To whom correspondence should be addressed: Gernot Längst and Attila Németh, Biochemistry Center Regensburg, University of Regensburg, Universitätsstr. 31, 93053 Regensburg, Germany. Tel.:

49-(0)941-943 2849; Fax: 49-(0)941-943 2474; E-mail: gernot.laengst@vkl.uni-regensburg.de, attila.nemeth@vkl.uni-regensburg.de

[2]Department of Molecular Epigenetics, Helmholtz Center Munich and Center of Integrated Protein Science Munich (CIPSM), 81377 Munich, Germany

[3]Adolf-Butenandt Institute and Munich Center of Integrated Protein Science (CIPSM), Ludwig Maximilians University of Munich, 80336 Munich, Germany

[4]School of Medicine, Flinders University, Adelaide 5001, Australia

[5]Diamantina Institute for Cancer, Immunology and Metabolic Medicine, University of Queensland Research Wing, Building 1, Princess Alexandra Hospital Campus, Ipswich Road, Buranda, Queensland 4102 Australia

[6]Department of Biology and Center for Integrated Protein Science, Ludwig Maximilians University of Munich, Grosshaderner Str. 2, 82152 Planegg-Martinsried, Germany

[7]The Netherlands Cancer Institute, Plesmanlaan 121, 1066 CX Amsterdam, The Netherlands

[8]The abbreviations used are: 5'ETS, 5' external transcribed spacer; AhR, aromatic hydrocarbon receptor; Mybbp1a, Myb-binding Protein 1a; PGC-1α, PPAR gamma coactivator 1α; PIC, pre-initiation complex; pre-rRNA, rRNA precursor; rDNA, rRNA gene; RNA Pol I, RNA Polymerase I; rRNA, ribosomal RNA; TTF-I -Transcription Termination Factor-I; t-Utps, transcriptional-Utps; Utps, U three proteins

FIGURE LEGENDS

FIGURE 1. Characterisation of the subcellular localization of Mybbp1a and its interaction with RNA Pol I. A. Control MB III cells and MB III cells stably expressing Flag-RPA116 (Flag-RPA116-MB III) were incubated with α-RPA116 (green) and α-Flag (red) antibodies to detect the endogenous and tagged RPA116 proteins and analyzed by phase contrast and immunofluorescence microscopy. A larger field is shown (right). B. Flag-RPA116-containing complexes were immunoprecipitated with α-Flag agarose from nuclear extracts of control MB III and Flag-RPA116-MB III cells. Load (L; 6%), flow-through (FT; 6%) and eluted proteins (E) were analyzed by Western blotting with the indicated antibodies. C. Flag-RPA116-containing complexes were immunoprecipitated with α-Flag agarose from whole cell extracts of MB III and Flag-RPA116-MB III cells. For the detection with α-RPA116 and α-Flag load (L, 40%), flow-through (FT, 40%), bead-bound (B) and eluted (E) proteins were analyzed by Western blotting. For the detection with α-Mybbp1a antibodies 0,8% of the load and flowthrough were loaded on the gel. D. Schematic representation of structural features of human Mybbp1a and its proteolytic cleavage products p140^{MBP} and p67^{MBP}. Mybbp1a contains several potential leucine charged domain motifs (Δ), basic amino acid repeats (*), an acidic domain (black box) and 2 highly conserved regions (CR) 1 and 2 harbouring several strictly conserved polar residues (31,46). Sequence analysis of Mybbp1a (ref AF147709.1) with the Conserved Domain database search (70) (version v.2.22) revealed two conserved domains: the DNA polymerase phi domain (DNA pol phi; pfam 04931; E-value: 1,54e-138) and the transcription initiation factor IIF alpha subunit (TFIIF-a; pfam 05793; E-value: 6,55e-03). Upon transcription impairment by chemical stress Mybbp1a gets partially proteolyzed to generate the N-terminal fragments p140^{MBP} and p67^{MBP} (44). NLS: Nuclear Localisation Signal (24). E. Localization Mybbp1a in HeLa cells. 48 h after transfection with human Flag-hMybbp1a, mouse Flag-mMybbp1a and mouse Flag-p67^{MBP}*NLS (Flag-mp67^{MBP}*) expression constructs cells were fixed and stained with the antibodies indicated on top. Co-localization is indicated by the orange colour. Non-transfected HeLa cells stained with α-Mybbp1a recognizing endogenous Mybbp1a are shown on the right. The positions of the nucleoli are indicated by arrows. F. Subnuclear localization of Mybbp1a in relation to nucleolar marker proteins analyzed with super-resolution structured illumination microscopy (71). Co-immunofluorescence staining of HeLa cells with anti-Mybbp1a antibody vs anti-B23 antibody (granular component, top panel), anti-fibrillarin antibody (dense fibrillar component, middle panel) and GFP-RPA43 (fibrillar center, bottom panel). DNA was counterstained with 4',6-diamidino-2-phenylindole (DAPI). Mid-section with conventional optical resolution are shown for comparison (left column). Scale bars: 5 µm and 0.5 µm (inset).

FIGURE 2. Mybbp1a represses rRNA gene transcription. A. Nuclear extracts of HEK239T cells either transfected with Flag-Mybbp1a expression plasmid (lanes 4 to 6) or control DNA (ctrl; lanes 1

to 3) were incubated with α-Flag agarose. For the detection with α-Mybbp1a and α-Snf2h load (L, 5%), flow-through (FT, 5%), bead bound (B) and eluted (E) proteins were analyzed by Western blotting. For the detection with α-PAF53 0.3% of the load and flowthrough were loaded on the gel. B. The pHrD-IRES-Luc (41) construct contains the human rDNA (hrDNA) promoter from -410 to + 314 (relative to the transcription start site) followed by an internal ribosome entry site (IRES) fused to the firefly luciferase coding region. The renilla control construct carrying the renilla luciferase gene under the control of a TK promoter (transcribed by Pol II) was used to normalize for transfection efficiency. C. HeLa cells were co-transfected with both luciferase reporter constructs, pHrD-IRES-Luc and renilla control, and increasing amounts (188 ng, 375 ng, 750 ng) of either human Mybbp1a, mouse Mybbp1a or Tip5 expression plasmids. The mouse $p67^{MBP}$*NLS (p67) expression plasmid was transfected with an amount of 188 ng. 48 h after transfection luciferase activity was measured and firefly luciferase counts (RNA Pol I reporter) were normalized to renilla luciferase counts and compared to the control transfection reaction (ctrl). Protein levels were analyzed by Western blotting with α-Flag antibody. An unspecific band (*) served as loading control. D. ChIP experiments were performed with chromatin derived from purified nucleoli (left) or whole cell extracts (right) of cells either transfected with human Flag-Mybbp1a expression plasmid (Flag-hMybbp1a) or control DNA (ctrl). For immuno-precipitation α-Flag, α-hMybbp1a, α-RPA116 and α-TTF-I were used as indicated. An α-IgG antibody was used for background estimation. Flag-hMybbp1a protein levels were analyzed by Western blotting with α-Mybbp1a and α-Flag antibodies as indicated.

FIGURE 3. Mybbp1a overexpression perturbs rRNA processing. A. Schematic representation of the rRNA processing in human cells (for more details see (52)). Intermediates and final processing products are shown. ETS: external transcribed spacer; ITS: internal transcribed spacer. A circle and a star indicate the locations of qRT-PCR and Northern probes. B. HeLa cells were transfected with increasing amounts of Flag-Mybbp1a expression plasmid or control DNA. Steady state levels of the 5'ETS were quantified in duplicate qRT-PCR measurements and normalized to b-actin mRNA levels. The upper diagram shows the average and standard deviation values, the middle and lower panels illustrate the overexpression of Mybbp1a by Western blot and immunofluorescence, respectively. C. rRNAs were detected on Northern blots after Mybbp1a overexpression in HeLa cells (upper panels). EtBr staining shows the mature 18S and 28S rRNA in the middle panel and Western blot shows in the lower panel the expression of Flag-Mybbp1a of three independent experiments. D. Quantification of the Northern blot shown in C. rRNA levels were normalized to 18S rRNA and expressed relative to the control reaction (ctrl). Averages and minimum and maximum values are shown. Two-tailed, paired t-tests were performed on the datasets and they showed that $p < 0.05$ in all cases ($p=0.02$ for 47S, $p=0.039$ for 41S, $p=0.011$ for 30S and $p=0.036$ for 21S).

FIGURE 4. Mybbp1a is part of a RNA-sensitive protein complex. A. RNase A-treated and mock-treated (ctrl) HeLa nuclear extracts were separated on a Superose 6 gelfitration column. Load (9%) and collected fractions (every second fraction from 12 to 34) were analyzed by Western blotting with the indicated antibodies. B. Nuclear extracts of HeLa cells either transfected with Flag-Mybbp1a expression plasmid (lane 5 - 8) or control DNA (ctrl; lane 1 - 4) were incubated with α-Flag agarose. Load (L; 5%), flowthrough (FT; 5%), bead-bound (B) and eluted proteins (E) were analyzed by Western blotting with the indicated antibodies. C. Polysome fractionation was performed on a sucrose gradient and Mybbp1a and Pes1 protein levels of the fractions were detected by immunoblotting. Pre-assembled ribosomal subunit, monosome and polysome fractions were detected by measuring UV absorbance at 254 nm as indicated. D. Nuclear extracts of HeLa cells either transfected with Flag-Mybbp1a expression plasmid or control DNA (ctrl) were used for immunoprecipitation with α-Flag agarose. Eluted protein fractions were separated by SDS-PAGE, silver stained, protein bands were cut and subjected to MALDI-TOF mass spectrometry. Proteins identified are indicated and their participation in ribosome biogenesis is summarized on the right.

FIGURE 5. siRNA-mediated depletion of Mybbp1a delays cellular proliferation. A. HeLa cells were transfected with siRNA targeting Mybbp1a (Mybbp1a.2), TIF-IA and a control siRNA (si-ctrl). Protein levels were analyzed by Western blotting 2, 4, 7, 9 and 12 days after transfection, as indicated. The α-tubulin staining of the membrane served as loading control. B. Cellular proliferation upon siRNA treatment of the cells, using si-Mybbp1a (white triangle), si-TIF-IA (white square) or si-ctrl

(black square), was followed from days 0 to 12 by counting the number of living cells. Cell numbers are plotted in log10 scale. The average and standard deviation values were calculated from three technical replicates. One of two independent data sets is shown.

Figure 1

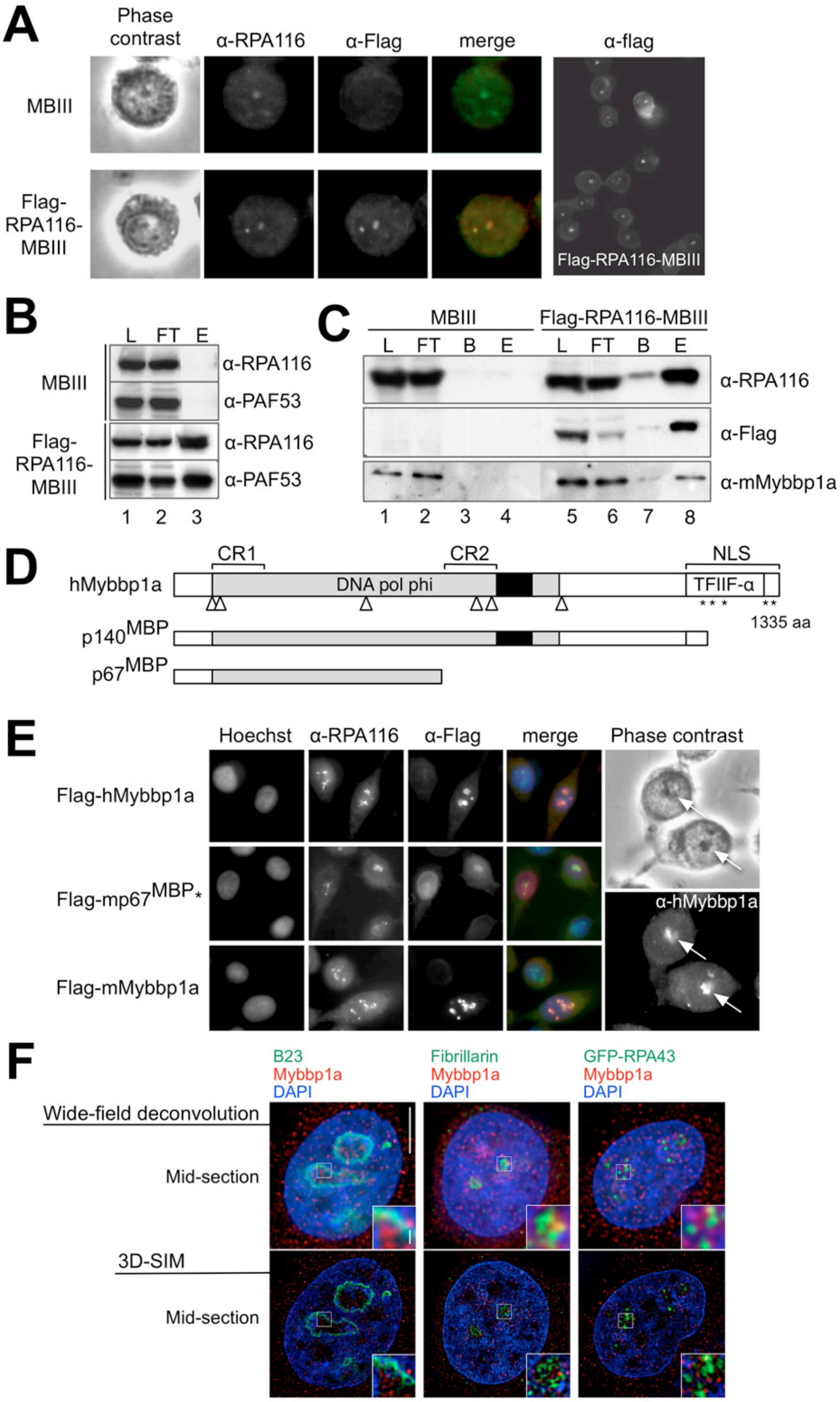
A
Phase contrast
α-RPA116
α-Flag
merge
α-flag
MBIII
Flag-RPA116-MBIII
Flag-RPA116-MBIII
B
L FT E
MBIII
Flag-RPA116-MBIII
α-RPA116
α-PAF53
α-RPA116
α-PAF53
1 2 3
C
MBIII
Flag-RPA116-MBIII
L FT B E L FT B E
α-RPA116
α-Flag
α-mMybbp1a
1 2 3 4 5 6 7 8
D
CR1
CR2
NLS
hMybbp1a
DNA pol phi
TFIIF-α
*** **
1335 aa
p140MBP
p67MBP
E
Hoechst
α-RPA116
α-Flag
merge
Phase contrast
Flag-hMybbp1a
Flag-mp67MBP*
Flag-mMybbp1a
α-hMybbp1a
F
B23
Mybbp1a
DAPI
Fibrillarin
Mybbp1a
DAPI
GFP-RPA43
Mybbp1a
DAPI
Wide-field deconvolution
Mid-section
3D-SIM
Mid-section

Figure 2

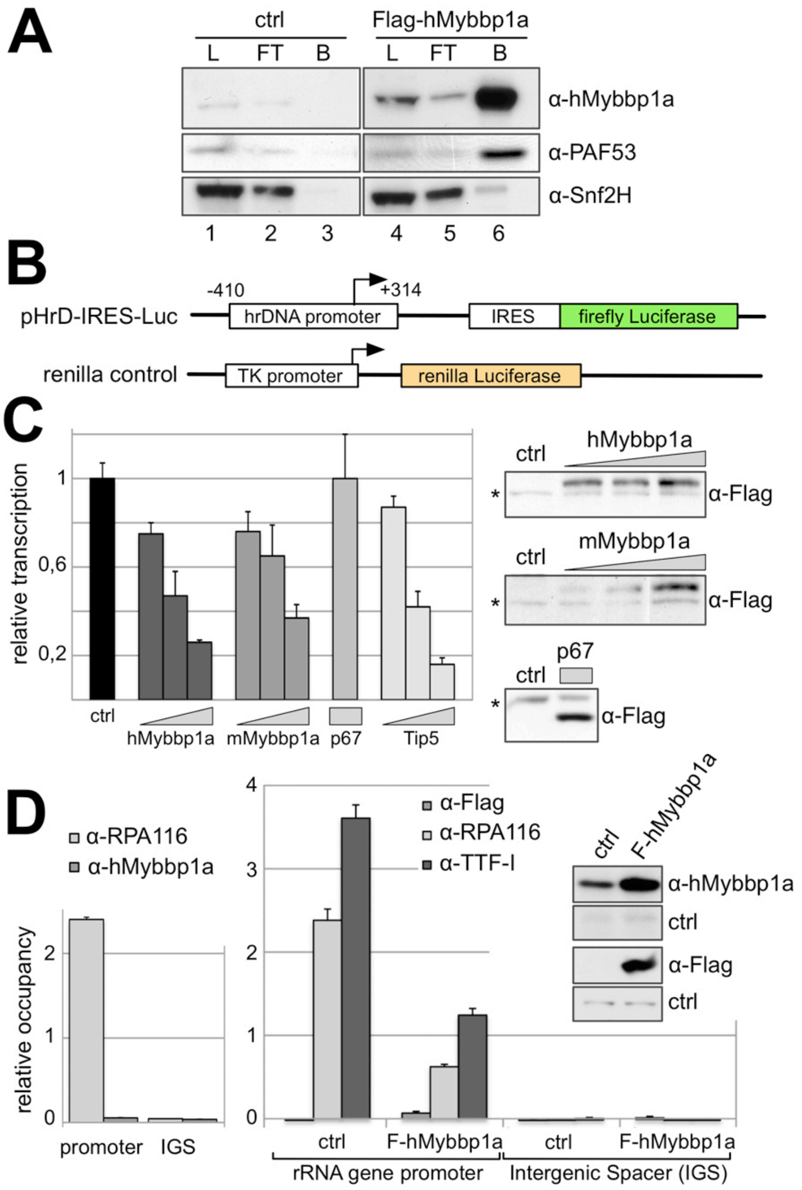
A
ctrl
Flag-hMybbp1a
L
FT
B
L
FT
B
α-hMybbp1a
α-PAF53
α-Snf2H
1
2
3
4
5
6
B
pHrD-IRES-Luc
-410
+314
hrDNA promoter
IRES
firefly Luciferase
renilla control
TK promoter
renilla Luciferase
C
relative transcription
1
0,6
0,2
ctrl
hMybbp1a
mMybbp1a
p67
Tip5
ctrl
hMybbp1a
*
α-Flag
ctrl
mMybbp1a
*
α-Flag
ctrl
p67
*
α-Flag
D
α-RPA116
α-hMybbp1a
relative occupancy
2
1
0
promoter
IGS
4
3
2
1
0
α-Flag
α-RPA116
α-TTF-I
ctrl
F-hMybbp1a
ctrl
F-hMybbp1a
rRNA gene promoter
Intergenic Spacer (IGS)
ctrl
F-hMybbp1a
α-hMybbp1a
ctrl
α-Flag
ctrl

Figure 3

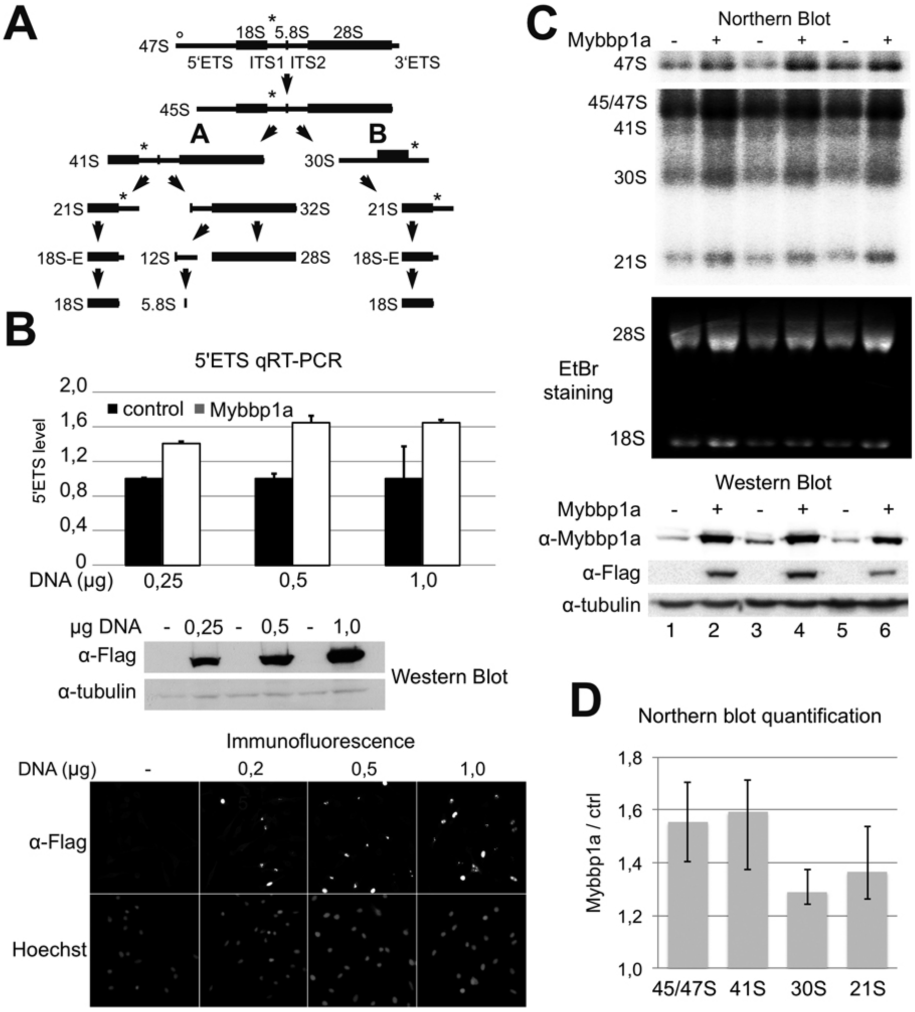
A
47S
18S
5.8S
28S
5'ETS
ITS1
ITS2
3'ETS
45S
A
B
41S
30S
21S
32S
21S
18S-E
12S
28S
18S-E
18S
5.8S
18S
B
5'ETS qRT-PCR
control
Mybbp1a
5'ETS level
2,0
1,6
1,2
0,8
0,4
0
DNA (µg)
0,25
0,5
1,0
µg DNA
-
0,25
-
0,5
-
1,0
α-Flag
α-tubulin
Western Blot
Immunofluorescence
DNA (µg)
-
0,2
0,5
1,0
α-Flag
Hoechst
C
Northern Blot
Mybbp1a
- + - + - +
47S
45/47S
41S
30S
21S
28S
EtBr staining
18S
Western Blot
Mybbp1a
- + - + - +
α-Mybbp1a
α-Flag
α-tubulin
1 2 3 4 5 6
D
Northern blot quantification
Mybbp1a / ctrl
1,8
1,6
1,4
1,2
1,0
45/47S
41S
30S
21S

Figure 4

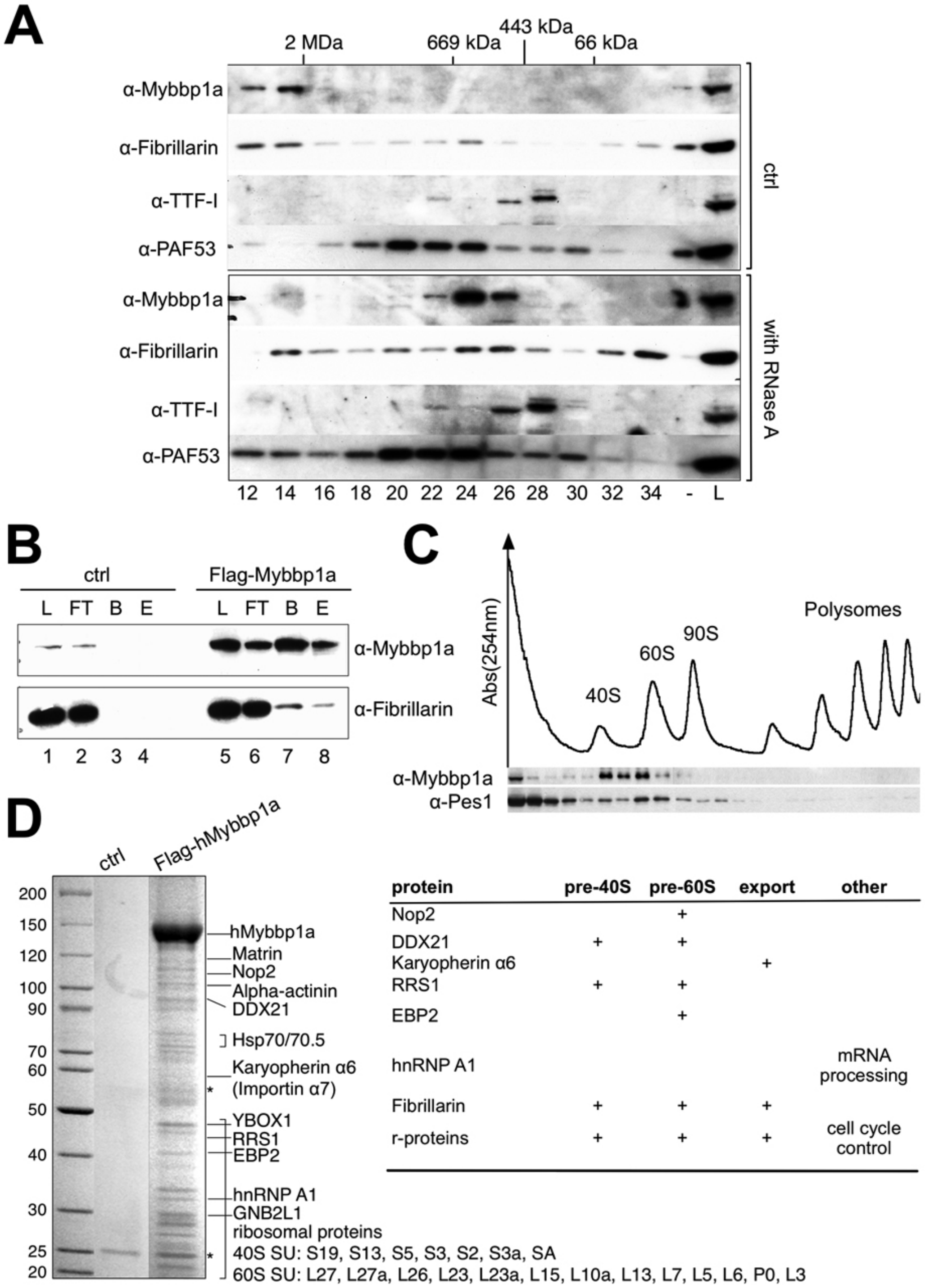

protein	**pre-40S**	**pre-60S**	**export**	**other**
Nop2		+		
DDX21	+	+		
Karyopherin α6			+	
RRS1	+	+		
EBP2		+		
hnRNP A1				mRNA processing
Fibrillarin	+	+	+	
r-proteins	+	+	+	cell cycle control

Figure 5

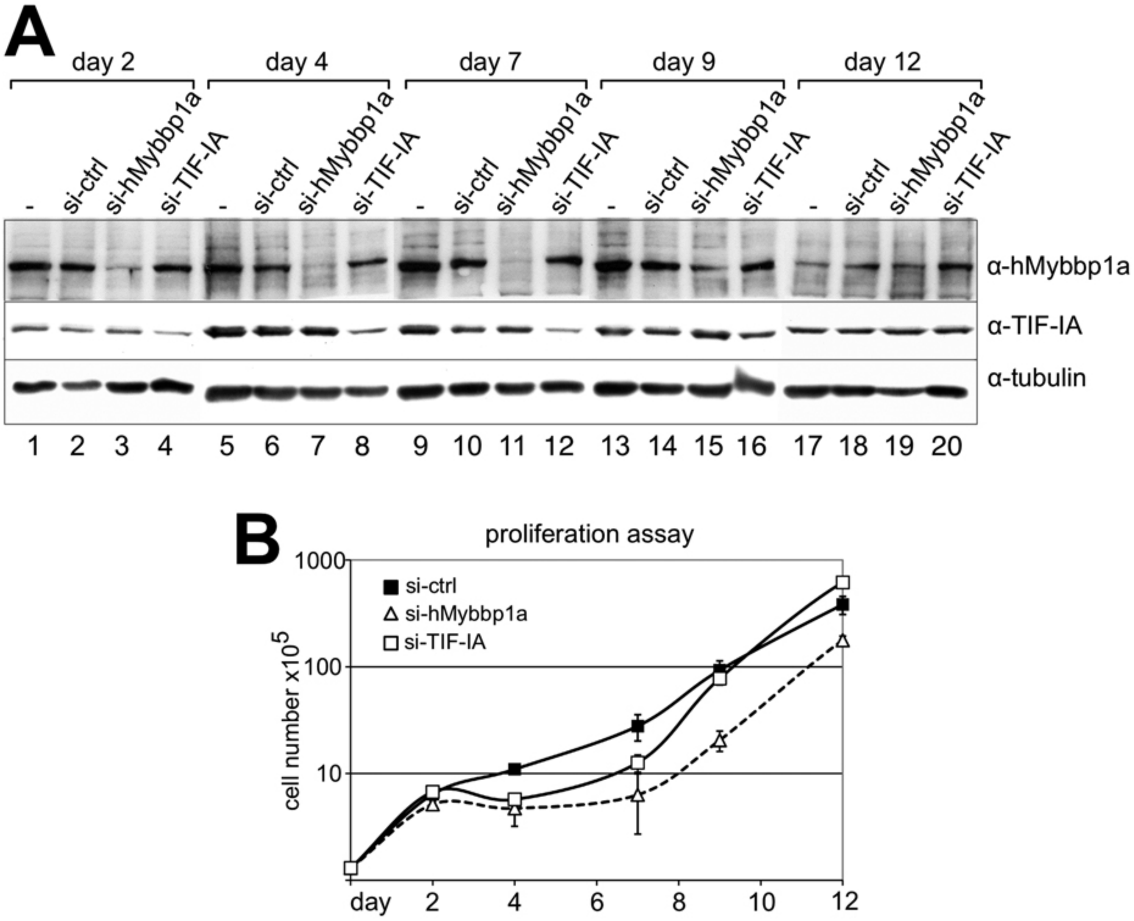
A
day 2
day 4
day 7
day 9
day 12
-
si-ctrl
si-hMybbp1a
si-TIF-IA
α-hMybbp1a
α-TIF-IA
α-tubulin
1 2 3 4 5 6 7 8 9 10 11 12 13 14 15 16 17 18 19 20
B
proliferation assay
■ si-ctrl
△ si-hMybbp1a
□ si-TIF-IA
cell number x10^5
1000
100
10
day
2
4
6
8
10
12